Sapphirine + Forsterite and Sapphirine + Humite-Group Minerals in an Ultra-Magnesian Lens from Kuhi-lal, SW Pamirs, Tajikistan: Are these Assemblages Forbidden?

by EDWARD S. GREW[1], NIKOLAY N. PERTSEV,[2]
MARTIN G. YATES[1], ANDREW G. CHRISTY[3],
NICHOLAS MARQUEZ[4], AND JOSEPH V. CHERNOSKY[1]

[1]*Department of Geological Sciences, University of Maine, 5711 Boardman Hall, Orono, Maine 04469-5711, USA*
[2]*Institute of Geology of Ore Deposits, Petrology, Mineralogy, and Geochemistry of the Russian Academy of Sciences, Staromonetny per., 35, Moscow 109017, Russia*
[3]*Department of Chemistry, University of Leicester, Leicester LE1 7RH, UK*
[4]*Aerospace Corporation, P.O. Box 92957, Los Angeles, California 90009, USA*

(Received 26 March 1993; revised typescript accepted 19 November 1993)

ABSTRACT

Sapphirine occurs with humite-group minerals and forsterite in Precambrian amphibole-facies rocks at Kuhi-lal, SW Pamir Mountains, Tajikistan, a locality also for talc + kyanite $\pm$ magnesiohornblende whiteschist. Most of these sapphirine-bearing rocks are graphitic and sulfidic (pyrite and pyrrhotite) and contain enstatite, clinohumite or chondrodite, spinel, rutile, gedrite, and phlogopite. A phlogopite schist has the assemblage with $X_{Fe} = Fe/(Fe + Mg)$ increasing as follows: chlorite (0·003) < phlogopite (0·004–0·005) $\leqslant$ sapphirine (0·004–0·006) $\leqslant$ enstatite (0·006) $\leqslant$ forsterite (0·006–0·007) < spinel (0·014). This assemblage includes the incompatible pair sapphirine + forsterite, but there is no textural evidence for reaction. In one rock with clinohumite, X_{Fe} increases as follows: clinohumite (0·002) < sapphirine (0·003) < enstatite (0·004–0·006) < spinel (0·010). Ion microprobe and wet-chemical analyses give 0·57–0·73 wt.% F in phlogopite and 0·27 wt.% F in chlorite in the phlogopite schist; 0·04, 1·5–1·9, and 4·4 wt.% F in forsterite, clinohumite, and chondrodite, respectively; and 0–0·09 wt.% BeO and 0·05–0·21 wt.% B_2O_3 in sapphirine. Stabilization of sapphirine + clinohumite or sapphirine + chondrodite instead of sapphirine + phlogopite is possible at high F contents in K-poor rocks, but minor element contents appear to be too low to stabilize sapphirine as an additional phase with forsterite + enstatite + spinel. Although sapphirine + forsterite is metastable relative to spinel + enstatite in experiments conducted at $a_{H_2O} = 1$ in the $MgO–Al_2O_3–SiO_2–H_2O$ system, it might be stabilized at $a_{H_2O} \approx 0·5$, $P \leqslant 4$ kbar, $T \approx 650–700°C$. Textures in the Kuhi-lal whiteschists suggest a polymetamorphic evolution in which the rocks were originally metamorphosed at $T \geqslant 650°C$, $P \geqslant 7$ kbar, conditions under which sapphirine + clinohumite and sapphirine + chondrodite are inferred to have formed, and subsequently affected by a later event at lower P, similar T, and lower a_{H_2O}. The latter conditions were favorable for sapphirine + forsterite to form in a rock originally containing chlorite + forsterite + spinel + enstatite.

INTRODUCTION

Sapphirine, an Al-rich chain silicate with the structural formula $(Mg,Fe^{2+},Fe^{3+},Al)_8O_2(Al,Si)_6O_{18}$, typically occurs in aluminous rocks metamorphosed under conditions of the upper amphibolite and granulite facies [reviewed by Deer *et al.*

(1978)]. It is commonly associated with other Al-rich minerals such as cordierite, sillimanite, corundum, and spinel, as well as with two minerals relatively poor in Al, orthopyroxene and phlogopite. Associations with other Al-poor ferromagnesian minerals are much less common: for example, assemblages of sapphirine + forsterite and sapphirine + a humite-group mineral have been described only from the four localities listed in Table 1.

Lal *et al.* (1978) suggested that F stabilized assemblages of humite group minerals + sapphirine in rocks from Assam, India. However, there is no obvious explanation for the assemblage sapphirine + forsterite, because in the system $MgO–Al_2O_3–SiO_2$, sapphirine + forsterite is incompatible with the assemblage enstatite + spinel (Fig. 1), the latter being reported from many sapphirine-bearing rocks. Sapphirine + forsterite has not been reported to be stable in any experimental studies, whereas enstatite + spinel is reported to be stable from 765 to 1565 °C and from 1·5 to 20 kbar (Taylor, 1973; Seifert, 1974; Herzberg, 1983; Liu & Presnall, 1990).

In the present paper, we describe assemblages from Kuhi-lal, Tajikistan, with sapphirine + forsterite and sapphirine + a humite-group mineral and consider possible chemical and microstructural controls on their stability. Although substantial F can explain stabilization of sapphirine + clinohumite or chondrodite at Kuhi-lal, the amounts of minor constituents in the Kuhi-lal sapphirine + forsterite rock appear to have been insufficient to have stabilized this assemblage instead of (or together with) enstatite + spinel. A difference in structural state or degree of cation order between natural and synthetic sapphirine (e.g., Newton *et al.*, 1974; Kiselyova, 1976), an alternative explanation that we had considered earlier (Grew *et al.*, 1991), no longer appears to be viable. Christy *et al.* (1992) reported no significant differences in cation order between natural and synthetic sapphirine, and the present study revealed no anomalous microstructural features in either sapphirine or forsterite (A. G. Christy, unpub. data, 1992). Instead, we propose that the assemblage sapphirine + forsterite is stabilized at water activities (a_{H_2O}) substantially lower than those at which Seifert (1974) conducted his experiments.

GEOLOGIC FRAMEWORK

Ultra-magnesian rocks, including the sapphirine-bearing rocks described here, as well as the sapphirine-bearing rocks (no orthosilicate) reported by Zotov (1966) and Zotov & Sidorenko (1968), form a 1 km × 1·5 km lens in pelitic biotite gneiss at Kuhi-lal, a village situated on the Tajikistan side of the Pyanj River (Fig. 2). Other ultra-magnesian rocks at Kuhi-lal are magnesite marble, relatively coarse-grained rocks containing amphibole, enstatite, spinel, forsterite, and humite-group minerals, and schists containing talc, amphibole, and phlogopite, including whiteschist (talc + kyanite assemblage, Budanova, 1987; Grew *et al.*, 1988, 1990b). Dolomite and calcite marbles are also present. The origin of the ultra-magnesian rocks, e.g., whether by isochemical metamorphism of highly magnesian precursors, synmetamorphic metasomatism involving plutonic activity or tectonic insertion, or by partial melting, is a debatable question that is beyond the scope of the present paper.

A characteristic mineral assemblage in the pelitic country rocks overlying the ultra-magnesian lens at Kuhi-lal is fibrolitic sillimanite (± kyanite, probably relict) + K-feldspar + quartz + plagioclase + biotite ± garnet. Overall, the presence of both kyanite and sillimanite with K-feldspar is characteristic of the Goran series (Drugova *et al.*, 1976).

The Goran series, which includes some 10 ultra-magnesian lenses such as that at Kuhi-lal (e.g., Kiselyov & Budanov, 1986), is part of a crystalline complex extending from the southwestern Pamirs to Sar-e-Sang (Fig. 2), the type locality for whiteschists (Schreyer,

TABLE 1

Localities for sapphirine + orthosilicate assemblages

Locality*	Assemblage	T(°C)/P(kbar)	Orthosilicate F	Spr FeO	Spr B_2O_3
	Assemblages with humite-group minerals				
1. Assam (India)	Spr + Nrb + Spl + Phl + Ilm + Rt	700–800/5–6	11·2	2·8	—
1. Assam (India)	Spr + Hu + Spl + Ged + Ilm + Rt	700–800/5–6	4·5	3·4	—
2. Kuhi-lal (Tajik.)	Spr + Chn + En + Rt + Po(+Py) + Gr	≥650/≥7	4·4	0·2–0·3	0·05
2. Kuhi-lal (Tajik.)	Spr + Chu + Spl + En ± Rt + Po(+Py) ± Gr	≥650/≥7	1·5–1·9	0·1–0·2	0·1–0·2
	Assemblages with forsterite				
3. Mojave Desert (USA)	Spr + Fo + Spl + Di + Phl + Cal + Dol + Rt	800–850/7·5–9	—	1·3	—
4. Napier Mtns. (Antarctica)	Spr + Fo + Spl + En + Phl	850/5	—	≈2·0†	—
2. Kuhi-lal (Tajik.)	Spr + Fo + Spl + En + Phl + Chl ± Po	≤675/≤4	0·04	0·2	0·2

* Sources: 1—Lal et al. (1978). 2—Grew et al. (1988, 1990b, 1991); this study; cf. original P estimate of 6·2–6·5 kbar for the decompression event. 3—Henry & Dokka (1992). 4—Ravich & Kamenev (1972); Harley & Hensen (1990).

† Estimated from the refractive indices reported by Ravich & Kamenev (1972, table 43, no. 208L), namely $\gamma = 1·710$, $\alpha = 1·704$, and Sahama et al.'s (1974) table 2 and fig. 7.

Abbreviations: Cal—calcite, Chl—chlorite, Chn—chondrodite, Chu—clinohumite, Di—diopside, Dol—dolomite, En—enstatite, Fo—forsterite, Ged—gedrite, Gr—graphite, Hu—humite, Ilm—ilmenite, Nrb—norbergite, Phl—phlogopite, Po—pyrrhotite, Py—pyrite, Rt—rutile, Spl—spinel, Spr—sapphirine. The humite-group minerals are approximately $Mg(OH,F)_2 \cdot nMg_2SiO_4$, where $n = 1$ for norbergite, $n = 2$ for chondrodite, $n = 3$ for humite, and $n = 4$ for clinohumite.
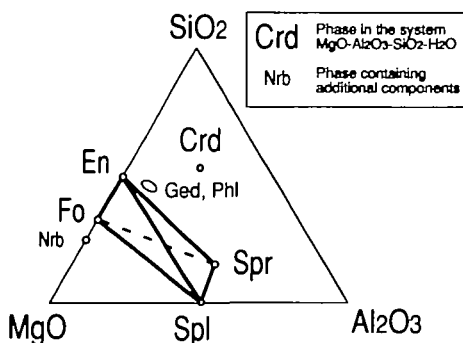
F IG. 1. Compositional plot in the model system $MgO-Al_2O_3-SiO_2$ illustrating the incompatibility of enstatite + spinel and sapphirine + forsterite. Clinohumite and chondrodite would plot between forsterite and norbergite. Abbreviations: Crd—cordierite, En—enstatite, Fo—forsterite, Ged—gedrite, Nrb—norbergite, Phl—phlogopite, Spr—sapphirine, Spl—spinel.

1977). At both Sar-e-Sang and Kuhi-lal, the whiteschists bear testimony to a polymetamorphic history (e.g., Schreyer & Abraham, 1976; Grew *et al.*, 1988). An early high-pressure event stabilized talc + kyanite + gedrite or hornblende at $P \geqslant 7$ kbar, $T = 630$–$670\,°C$; this was followed by a near-isothermal drop in pressure by at least 0·5 kbar that resulted in cordierite coronas around kyanite (Kulke & Schreyer, 1973; Grew, 1988; Grew *et al.*, 1988; Massonne, 1989). Andalusite at Kuhi-lal is inferred to have formed when pegmatites were emplaced during the Mesozoic (Grew *et al.*, 1988).

DESCRIPTION OF THE SAPPHIRINE + ORTHOSILICATE ROCKS

General statement

The sapphirine + orthosilicate rocks include two distinct types. The sapphirine + forsterite rock is a schist containing white phlogopite, whereas the rocks with sapphirine + clinohumite or chondrodite range from light gray to black (depending on amount of carbonaceous material and sulfide present) and from nearly unfoliated to well foliated.

Sapphirine + forsterite assemblage

Only one sample of sapphirine + forsterite was found: KL920A (Table 2, Fig. 3). It was collected from schists associated with a pegmatite near the locality for the talc + kyanite + magnesiohornblende rocks described by Grew *et al.* (1988). Prominent in hand specimen are crudely oriented, colorless phlogopite plates commonly 0·5–2 cm in diameter. In thin section, these coarse phlogopite flakes, in places kinked or wavy, and forsterite masses up to 1 cm long occur in a matrix of medium-grained, randomly oriented phlogopite and colorless, markedly birefringent chlorite (typically 0·2–1·5 mm long). Chlorite does not appear to be replacing phlogopite because the flakes of these minerals are rarely parallel. Spinel grains are mostly 0·1–1·5 mm in diameter and generally subhedral or euhedral; they are commonly clustered. Enstatite and sapphirine are less abundant. Sapphirine forms colorless, tabular grains mostly 0·3–1·5 mm long, noteworthy for their fine polysynthetic twinning. Enstatite prisms, up to 5 mm in length, locally have a lamellar structure. Overall, the major constituents in sample KL920A have been little affected by late alteration.

Although KL920A contains sapphirine + forsterite as well as spinel + enstatite, there is no textural evidence for a reaction between any of the phases present. Some forsterite + spinel
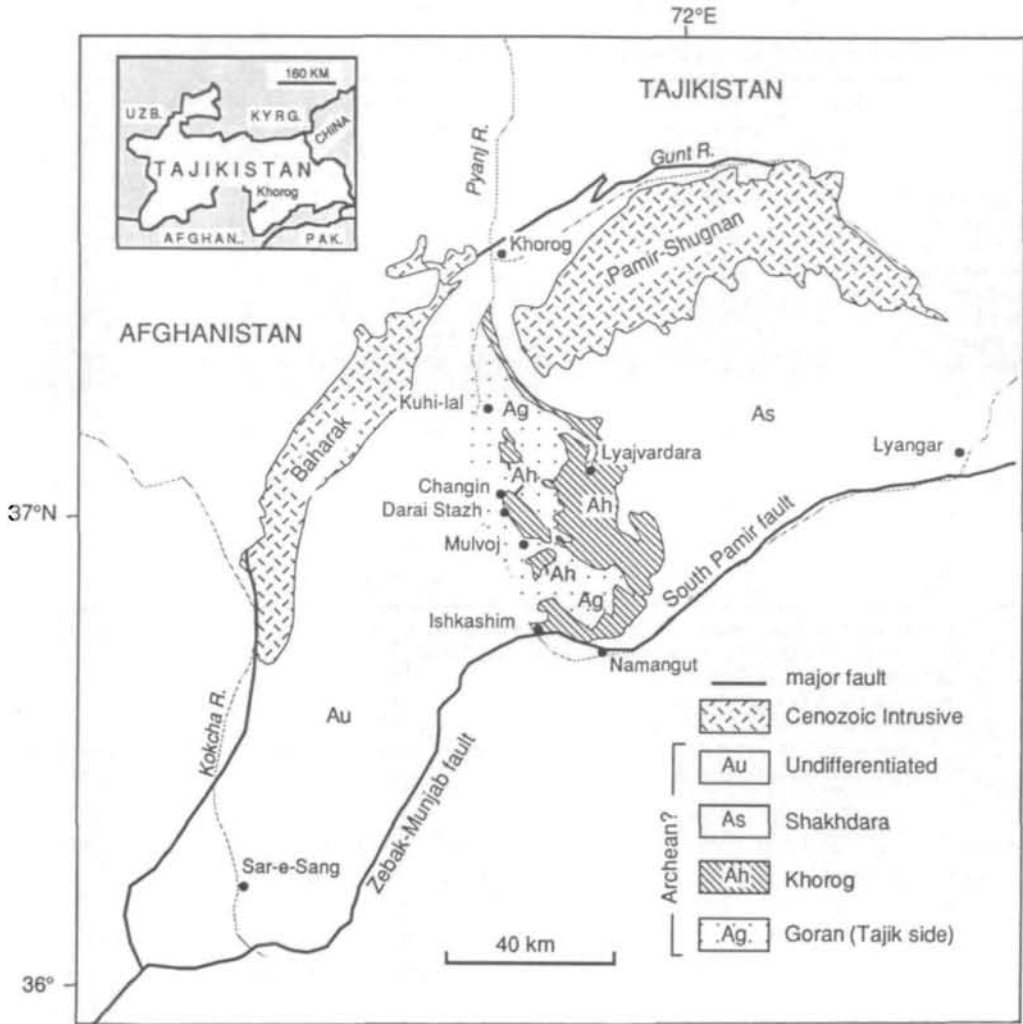
FIG. 2. Geologic map of the southwestern Pamir Mountains, Tajikistan, and of Badakhshan (NE Afghanistan), simplified from Vlasov & D'yakov (1989) with additional data from Desio *et al.* (1964), Desio (1975), and Shanin *et al.* (1979). For the Tajik side, the units include the Goran series (Ag) and the Shakhdara series, here separated into the Khorog suite (Ah) and the overlying suites, undifferentiated (As); for the Afghan side, undifferentiated Archean (Au). The Cenozoic ages for the intrusive rocks are taken from Desio (1975) and Shanin *et al.* (1979). Kuhi-lal, Changin, Darai Stazh, Mulvoj, and Ishkashim are localities for ultra-magnesian rocks in the Goran series.

patches include subordinate enstatite in physical contact with spinel (Fig. 3A). Other forsterite + spinel patches include sapphirine in physical contact with forsterite (Fig. 3B,C). One patch contains all four phases in which the closest approach between enstatite and sapphirine is 0·05 mm.

Sapphirine + clinohumite and sapphirine + chondrodite assemblages

Most of these rocks are relatively coarse grained and moderately foliated; sample KL940, a well-foliated and cherty rock, appears to be a mylonitized variety of the coarse-grained

TABLE 2

Mineralogy of the sapphirine + orthosilicate rocks from Kuhi-lal, Tajikistan

	KL920A in situ*	5164† dump*	5165† dump*	KL940 dump*	KL967 A‡ dump*	KL967 V‡ dump*	KL967 C‡ dump*	KL9266 core*	KL985 core*
Sapphirine	X	X	T	T	X	X	X	X	X
Forsterite	X§	—	—	—	—	—	—	—	—
Clinohumite	—	X§	X§	X§	X§	X§	X§	X§	—
Chondrodite	—	—	—	—	—	—	—	—	X§
Enstatite	X	X	X	X	X	X	X	X	X
Spinel	X	X	X	X	X	X	X	X	—
Gedrite	—	—	—	X	X	X	—	X	X
Phlogopite	X	T	T	T	T	T	—	X	—
Chlorite	X	T	T	T	T	—	—	—	T
Rutile	—	T	X	—	T	T	T	T	T
Rt + En symp.	—	T	T	T	T	T	T	T	T
Pyrrhotite	T	T	X	T	X	X	X	X	X
Pyrite	—	T	T	T	T	T	T	X	X
Graphite	—	X	—	—	X	X	X	X	X
Apatite	—	—	T	—	—	—	—	—	—
Zircon	—	—	T	—	T	T	—	—	—
Other (all T)	—	—	—	—	Unk	Mgs(?)	Unk	—	—

* *In situ* indicates that the sample was collected from bedrock; dump indicates that the sample was collected as a loose piece in a mine dump. Cores also collected in the mine dump.
† Sample collected by D. I. Belakovskiy.
‡ Refers to different sections cut from the same specimen.
§ Identification confirmed by X-ray diffraction (in the case of KL967, for sample as a whole).
X, major constituent; T, trace constituent. Rt + En symp.—symplectitic intergrowth of rutile and enstatite, Mgs—magnesite, Unk—unidentified secondary mineral.

sapphirine + clinohumite rocks. The most abundant ferromagnesian silicates and oxides are enstatite, clinohumite or chondrodite, spinel, sapphirine, and gedrite (Table 2).

In the unmylonitized rocks, enstatite forms prisms up to several centimeters long, which in places are oriented to give an indistinct foliation. In most sections (Table 2), vermicules of rutile are found in some enstatite margins bordering on clinohumite (Fig. 4A), and, in places, such enstatite–rutile symplectite forms discrete grains adjacent to clinohumite (Fig. 4B).

Clinohumite forms conspicuous yellow aggregates in a few of the samples. It is commonly pleochroic in yellow, as is chondrodite in KL985. Both minerals are twinned, and in many sections show little secondary alteration. Identification was confirmed by X-ray diffraction, and, in a few cases, by Raman spectroscopy (J. Pasteris & B. Wopenka, personal communication, 1991, 1992).

Sapphirine grains are colorless, commonly tabular, and, in part, subhedral or euhedral; in KL9266, sapphirine forms coarse, anhedral grains (Fig. 5). Polysynthetic twinning is characteristic of sapphirine in all the samples; simple penetration twins are also found. Sapphirine is in direct contact with clinohumite and chondrodite; a selvage of late, unidentified alteration material intervenes in KL9266.

Pyrrhotite is the dominant sulfide in the sapphirine + clinohumite and sapphirine + chondrodite rocks. It is generally anhedral, whereas pyrite ranges from anhedral to euhedral. In sample KL9266, pyrite forms a mantle around pyrrhotite. Graphite grains range in size from dust-like particles included in other minerals to well-defined flakes.

Gedrite, phlogopite (or mica resembling phlogopite), and chlorite appear to be secondary. Except in the mylonitized rocks, where textural relations are obscured, gedrite prisms penetrate enstatite, and in KL9266, sapphirine and clinohumite as well. Phlogopite and
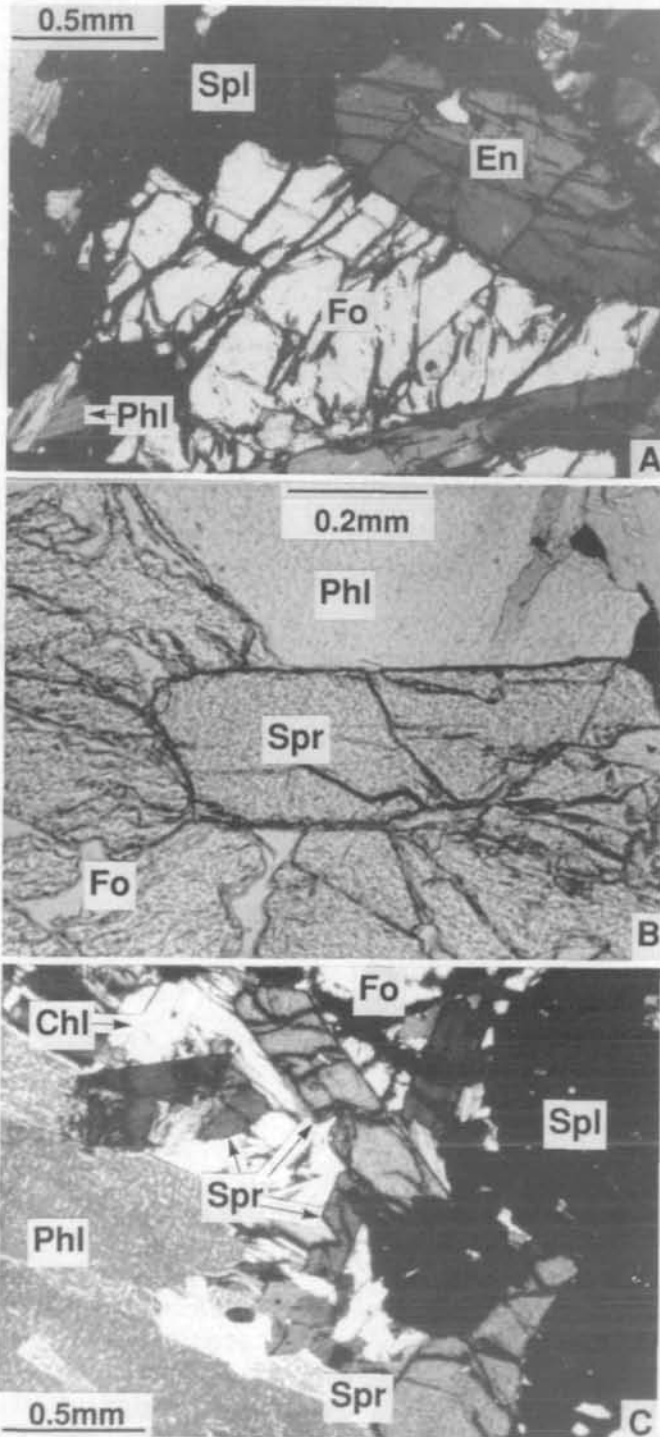
FIG. 3. Photomicrographs of sample KL920A. (A) Enstatite (En) in direct contact with forsterite (Fo) and spinel (Spl); phlogopite (Phl) also present. Crossed nicols. (B) Sapphirine (Spr) in direct contact with forsterite and phlogopite. Plane-polarized light. (C) Sapphirine with polysynthetic twinning with forsterite, phlogopite, spinel, and chlorite (Chl). Crossed nicols.
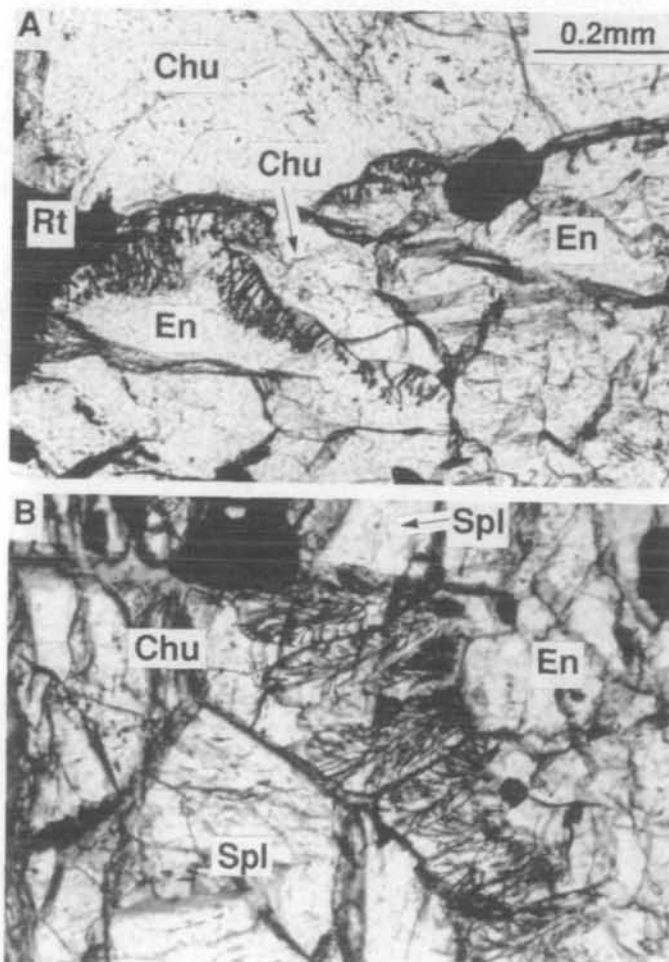
FIG. 4. Photomicrographs of sample 5165 showing enstatite–rutile symplectite. (A) Rutile vermicules in enstatite (En) along its contact with clinohumite (Chu). (B) Grains of enstatite–rutile symplectite between enstatite and clinohumite. Rt—Rutile. Plane-polarized light.

chlorite occur as inclusions in spinel (sample 5164) or in enstatite; phlogopite also occurs with gedrite, notably in KL9266.

CHEMICAL COMPOSITION

Methods

The minerals were analyzed at the University of Maine for major constituents with a MAC 400s electron microprobe (15 kV, 20–40 nA specimen current on quartz) equipped with TAP, PET, and LiF wavelength-dispersive spectrometers (WDS), as well as a LINK AN 10000 energy-dispersive system. The WDS data were corrected using the method of Bence & Albee (1968) and silicate and oxide standards of simple composition. One to six grains per thin section were analyzed at several spots each.

Li, Be, B, F, Rb, Sr, and Ba were analyzed with the ARL ion-microprobe mass analyzer at the Aerospace Corporation using the procedure of Grew *et al.* (1990a). One to three grains
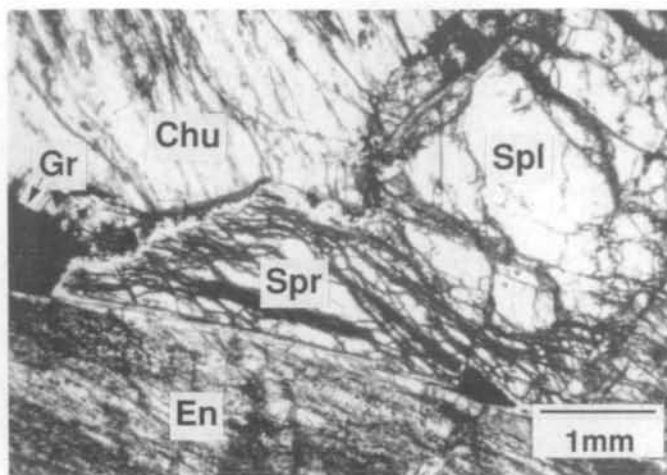
FIG. 5. Photomicrograph of sample KL9266 showing sapphirine (Spr), clinohumite (Chu), enstatite (En), graphitic aggregate (Gr), and spinel (Spl). Plane-polarized light.

each of sapphirine, forsterite, humite-group minerals, enstatite, and phlogopite per sample were analyzed with the ion microprobe. Most of the ion microprobe analyses were performed on a second set of sections mounted in Epotec 301 epoxy, because the epoxy used in mounting the first set of sections contained sufficient F to contaminate the ion microprobe analyses at levels of about $\leqslant 0.2$ wt.% F. The ion microprobe data on phlogopite in KL920A are in fair agreement with wet-chemical analyses on a coarse-grained phlogopite separate from this sample performed at XRAL Assay Laboratories, Don Mills, Ontario, Canada, where H_2O^+ was also analyzed (see Table 5, below).

Results

Clinohumite varies somewhat from section to section in Ti ($2.7–3.1$ wt.% TiO_2), whereas chondrodite is heterogeneous in a single section ($2.5–3.7$ wt.% TiO_2); FeO contents for both do not exceed 0.4 wt.% (e.g., Table 3). The analyses were recast into the formula $n[M_2SiO_4] \cdot [M_{1-x}Ti_x(OH,F)_{2-2x}O_{2x}]$, where M = Mg, Fe, Mn (Deer et al., 1982), with $n = 4$ (clinohumite) for 5164, KL9266, and KL967A and $n = 2$ (chondrodite) for KL985.

Sapphirine and enstatite vary in Al_2O_3 content from grain to grain as well as from sample to sample along a trend close to Tschermak's substitution $MgSiAl_{-2}$ (Table 4, Fig. 6). Li, Be, B, F, and Sr are at or below ion microprobe detection limits in enstatite (FeO = $0.14–0.43$ wt.%), and Cr, V, and Zn contents are at or below electron microprobe detection limits in spinel (FeO = $0.12–0.74$ wt.%).

Gedrite composition in sample KL9266 varies markedly from grain to grain and within individual grains in terms of the edenitic and Tschermak's substitutions. Phlogopite in KL920A is relatively homogeneous, and remarkable for its high Na content (Table 5).

Fractionation of Fe and Mg between the ferromagnesian minerals broadly follows trends reported elsewhere (e.g., Lal et al., 1978; Grew, 1988), although some ambiguity is introduced because of the reduced precision in measuring such low FeO contents. $X_{Fe} = Fe/(Fe + Mg)$ increases as follows: in KL920A, chlorite (0.003) < phlogopite ($0.004–0.005$) $\leqslant$ sapphirine ($0.004–0.006$) $\leqslant$ enstatite (0.006) $\leqslant$ forsterite ($0.006–0.007$) < spinel (0.014); in KL967A, clinohumite (0.002) < sapphirine (0.003) < enstatite ($0.004–0.006$) < spinel (0.010). In 5164 and KL9266, clinohumite is the most magnesian phase,

TABLE 3

Analyses of forsterite, clinohumite, and chondrodite

	Forsterite KL920A 6/3*	Clinohumite 5164 1/1*	Clinohumite KL9266 2/2*	Chondrodite KL985 2/1*
Electron microprobe wt.%				
SiO$_2$	42·33	38·38	38·32	34·56
TiO$_2$	0·05	2·97	2·68	3·22
Al$_2$O$_3$	<0·01	0·04	0·03	0·03
FeO	0·68	0·12	0·13	0·28
MnO	0	—	0	0
MgO	56·93	56·11	55·61	55·01
CaO	0·03	—	0·02	≤0·01
Ion microprobe wt.%				
Li$_2$O	0·001	0·001	0·001	0
B$_2$O$_3$	0·03	0·03	0·03	0·01
F	0·04	1·5	1·9	4·4
Calculated wt.%				
H$_2$O	—	1·49	1·35	2·31
O≡F	−0·02	−0·63	−0·80	−1·85
Total	100·07	100·01	99·27	97·97
Formulae				
O	4	17·233	17·211	9·142
Si	0·994	4·005	4·026	2·022
B	0·001	0·005	0·005	0·001
Ti	0·001	0·233	0·211	0·142
Al	0	0·005	0·004	0·002
Fe	0·013	0·010	0·011	0·013
Mg	1·994	8·730	8·709	4·798
Ca	0·001	—	0·002	0
Total cations	3·004	12·988	12·968	6·978
F	0·003	0·495	0·631	0·814
OH	—	1·039	0·947	0·902

* Number of electron microprobe analyses averaged/number grains in the average.

Formulae were calculated from $4[(Mg,Fe)_2SiO_4]\cdot[(Mg,Fe)_{1-x}Ti_x(OH,F)_{2-2x}O_{2x}]$ for clinohumite and $2[(Mg,Fe)_2SiO_4]\cdot[(Mg,Fe)_{1-x}Ti_x(OH,F)_{2-2x}O_{2x}]$ for chondrodite (Deer *et al.*, 1982).

whereas sequences of X_{Fe} among enstatite, sapphirine, and spinel vary. The sequence in KL985 appears to be anomalous: enstatite (0·002–0·003) < chondrodite (0·003–0·004) < sapphirine (0·004–0·006).

DISCUSSION

Interpretation of the assemblages

The overall assemblage in KL920A is forsterite + sapphirine + enstatite + spinel + chlorite + phlogopite ± pyrrhotite. Given the negligible iron and light-element contents, the first five phases could be described entirely by the system $MgO–Al_2O_3–SiO_2–H_2O$ (MASH), and this overall assemblage thus violates the phase rule. An alternative interpretation is to assume equilibrium was localized [cf. Korzhinskii's (1957) mosaic equilibrium] and consider the assemblages in different patches, i.e., forsterite + enstatite + spinel + chlorite and forsterite + sapphirine + spinel + chlorite. The relatively constant sapphirine compositions (Fig. 6) are consistent with the assumption that equilibrium was approached.

This patchwork of assemblages could have resulted from overprinting. In the associated

TABLE 4

Analyses of sapphirine

	KL920A 2/1*	5164 1/1*	KL9266 1/1*	KL985 1/1*
	Electron microprobe wt.%			
SiO_2	14·24	16·80	13·75	14·57
TiO_2	0·05	0·13	0·01	0·09
Al_2O_3	64·38	59·90	64·89	63·13
FeO	0·20	0·16	0·11	0·25
MnO	≤0·01	0·03	—	—
MgO	21·25	22·67	21·41	21·80
CaO	0·01	0·02	—	—
Na_2O	0·04	0·09	—	—
K_2O	—	0·01	—	—
	Ion microprobe wt.%			
Li_2O	0·002	0·002	0·001	0
BeO	0·009	0·09	0	0
B_2O_3	0·21	0·16	0·08	0·05
F	0	≤0·01	0	0
Total	100·39	100·06	100·25	99·89
	Formulae 20 O			
Si	1·629	1·927	1·576	1·677
Be	0·002	0·025	0	0
B	0·041	0·032	0·016	0·010
Al	8·680	8·096	8·768	8·566
Ti	0·004	0·011	0·001	0·008
Fe	0·019	0·015	0·011	0·024
Mn	0	0·003	—	—
Mg	3·624	3·876	3·659	3·742
Li	0·001	0·001	0	0
Ca	0·001	0·002	—	—
Na	0·009	0·020	—	—
K	—	0·001	—	—
Total	14·010	14·009	14·031	14·027

* Number of electron microprobe analyses averaged/number grains in the average.

whiteschists, overprinting of the earlier medium- to coarse-grained kyanite + magnesio-hornblende + talc assemblage resulted in coronas of relatively fine-grained cordierite, plagioclase, sapphirine, and corundum after decompression. In the case of sample KL920A, we suggest that the coarse-grained phlogopite crystallized during the event when kyanite + magnesiohornblende + talc formed, whereas the medium-grained phlogopite crystallized during the event following decompression when the coronas developed. Except for forsterite, the other minerals in KL920A are medium grained (Fig. 3), and a sequence of assemblages cannot be deduced from textures alone. Given the volume increase for the reaction En + Spl → Fo + Spr (see below), a logical sequence with decompression would be (1) forsterite + enstatite + spinel + chlorite, and (2) forsterite + sapphirine + spinel + chlorite. Conditions permitted the persistence of enstatite + spinel contacts in KL920A, and of kyanite relics in the whiteschists and pelitic gneisses.

The mineral assemblage inferred for 5164, 5165, KL940, KL967, and KL9266 is enstatite + spinel + clinohumite + sapphirine ± rutile ± graphite + pyrrhotite (+ pyrite) and for KL985, enstatite + chondrodite + sapphirine + rutile + graphite + pyrrhotite (+ pyrite). None of these assemblages violates the phase rule of C, F, S, and Ti are included with FeO, MgO, Al_2O_3, and SiO_2 as inert components. Figure 7 illustrates the difference between the two assemblages: the chondrodite assemblage implies a higher whole-rock F content. The
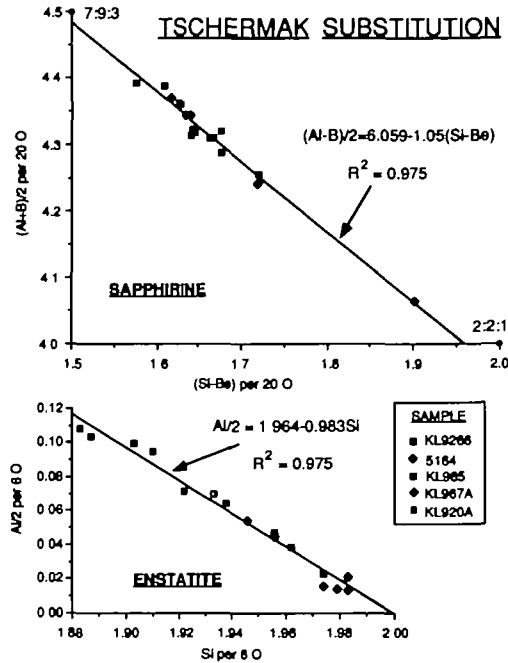
FIG. 6. Plot of sapphirine and enstatite compositions in terms of Al and Si. The ideal formulation for the Tschermak substitution in enstatite is $Al/2 = 2 - Si$, and in sapphirine, $Al/2 = 6 - 1.5$ Si with Si corrected for Be (Grew, 1981) and B combined with Al by analogy with kornerupine (Grew, 1988). The points 7:9:3 and 2:2:1 refer to the sapphirine compositions $Mg_7Al_{18}Si_3O_{40}$ and $Mg_2Al_4SiO_{10}$, respectively.

tie-line sapphirine + clinohumite pierces the triangle chondrodite + spinel + enstatite, a relationship that explains the absence of spinel in the assemblage with chondrodite (KL985).

Textural relations among sapphirine, spinel, enstatite, and clinohumite (e.g., KL9266, Fig. 5) are consistent with equilibrium crystallization of these four phases, presumably during the earlier event at $T \geqslant 650\,°C$, $P \geqslant 7$ kbar when talc + kyanite formed. On the other hand, the wide variation of enstatite and sapphirine compositions from grain to grain in some of the samples (Fig. 6) suggest disequilibrium, as do the vermicular rutile + enstatite intergrowths. Both features probably result from superposition of a later metamorphic event under lower-temperature conditions during which gedrite, together with minor fine-grained enstatite, phlogopite, and chlorite, formed from earlier sapphirine, enstatite, and clinohumite or chondrodite.

Factors stabilizing the Kuhi-lal sapphirine + orthosilicate assemblages

Microstructural, chemical, and thermodynamic factors could be invoked to explain the Kuhi-lal sapphirine + orthosilicate assemblages. However, transmission electron micro-scopy (TEM) study of individual minerals in five of the samples shows that there are no unusual microstructures. Sapphirine boron and Be (as well as Li) contents are relatively low, which implies that none of these constituents could have been responsible for stabilizing sapphirine as an additional phase. The Fe contents are too low for fractionation of Fe to stabilize sapphirine + humite-group mineral or sapphirine + forsterite with enstatite + spinel.

On the other hand, fluorine could have stabilized the assemblages sapphirine + humite-group minerals, as first suggested by Lal *et al.* (1978). If F is considered an inert component,

TABLE 5

Analyses of phlogopite and chlorite in KL920A

	Phlogopite* 3†	Chlorite 2†
Electron microprobe wt.%		
SiO_2	42·64	30·12
TiO_2	0·15	0·06
Al_2O_3	15·45	20·31
FeO	0·20	0·19
MnO	0	0
MgO	26·87	35·44
CaO	0	0·02
Na_2O	1·79	0
K_2O	7·97	0·03
Ion microprobe wt.%		
Li_2O	0·006	0
BeO	0	0
B_2O_3	0·006	0·006
Rb_2O	0·02	—
SrO	0·003	—
Cs_2O	0·002	—
BaO	0·05	—
F	0·57	0·27
Calculated		
H_2O	4·09	12·66
$O = F$	−0·24	−0·11
Total	99·58	99·00
Formulae		
Anion	20 O + 4OH	20 O + 16OH
Si	5·866	5·650
Al	2·133	2·348
B	0·001	0·002
Sum	8·0	8·0
Ti	0·015	0·008
Al	0·372	2·142
Fe	0·023	0·029
Mg	5·511	9·910
Li	0·003	0
Sum	5·924	12·089
Ca	0	0·004
Na	0·477	0
K	1·399	0·006
Rb	0·002	—
Ba	0·003	—
Sum	1·881	0·010
Total cations	15·805	20·099
F	0·248	0·160
OH	3·752	15·840

* Other methods gave (in wt.%): Li_2O 0·014 and Rb_2O 0·047 by atomic absorption, SrO 0·0035 and BaO 0·022 by inductively coupled plasma, B_2O_3 0·0055 by direct current plasma, F 0·73 by specific-ion electrode, and H_2O 5·5 by wet chemistry. X-ray powder data on coarse material gave $a = 5·302$ (5) Å, $b = 9·193$ (7) Å, $c = 10·186$ (8) Å, $\beta = 99°0$ (6)′, $V = 489·70$ (57) Å³, assuming a 1M unit cell.
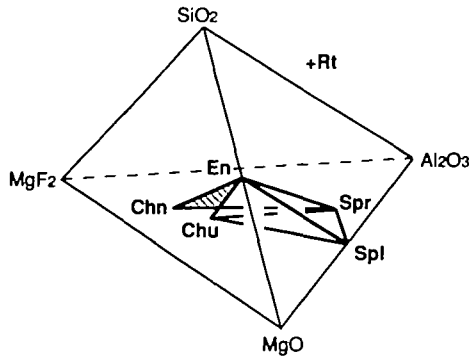
† Number of grains analyzed with the electron microprobe.

FIG. 7. Schematic projection through rutile into the $MgO-Al_2O_3-SiO_2-MgF_2$ system showing the sapphirine + clinohumite + enstatite + spinel (tetrahedron) and sapphirine + chondrodite + enstatite assemblages (hachured triangle, partly hidden). Abbreviations as in Table 1.

then the join sapphirine + humite-group mineral no longer intersects the join enstatite + spinel (Fig. 7). Indeed, assemblages with sapphirine and a humite-group mineral may be characteristic of F-rich, but Na- and K-poor, silica-undersaturated rocks metamorphosed under conditions of the upper amphibolite or granulite facies. Most silica-undersaturated, sapphirine-bearing rocks contain substantial K (and/or Na), thereby stabilizing phlogopite (and/or gedrite), both of which can accommodate considerable F.

However, F enrichment does not explain the sapphirine + forsterite assemblage at Kuhi-lal, where the forsterite contains only a trace of F. In this case, an explanation must be sought in the particular conditions of formation at Kuhi-lal. There is no experimental evidence for a stability field for sapphirine + forsterite at $a_{H_2O} = 1$. The petrogenetic grid developed by Seifert (1974) on the basis of experimental work precludes the stable coexistence of sapphirine + forsterite. Figure 8 shows a portion of Seifert's grid, which is a multisystem involving the phases Chl, Spr, Crd, Fo, En, and Spl (mineral abbreviations are given in Table 1). H_2O is assumed to be a fully mobile component. The Fo + Spr assemblage could only appear at a stable Chl-absent invariant point, that is, the intersection of the stable portions of the two Chl-absent univariant equilibria, En + Spr = Crd + Spl (Chl,Fo) and En + Spl = Fo + Crd (Chl,Spr). Seifert (1974) specifically carried our experiments to determine whether these two equilibria intersect, and he found that they were parallel within the uncertainties of his experimental data.

Nonetheless, the equilibria might intersect, if curvature resulting from the increase of enstatite Al_2O_3 content with temperature (e.g., Hensen & Essene, 1971; Berman, 1988) is taken into account. One alternative is that the stable portions of (Chl,Spr) and (Chl,Fo) intersect at high temperature. However, there is no experimental evidence for a sapphirine + forsterite field on the liquidus in the $MgO-Al_2O_3-SiO_2$ system at 1 bar (Foster, 1950; Keith & Schairer, 1952; Schreyer & Schairer, 1961; Smart & Glasser, 1976) or at 15 kbar (Taylor, 1973). The other alternative is that the metastable portions of (Chl,Spr) and (Chl,Fo) intersect at temperatures below [Spr] and [Fo]. If such an intersection exists, as is illustrated in Fig. 9, it would then be possible to reconcile Seifert's experiments with the natural occurrence of forsterite + sapphirine.

The first step is to consider water activity as an additional variable. In constructing Fig. 9, we have applied the approach which Hensen (1986) adopted to relate sapphirine assemblages formed at high and low oxygen fugacities in the Fe-Mg-Al-Si-O system. Seifert's experiments were carried out in the presence of an aqueous phase, so that $a_{H_2O} = 1$, whereas water activities in the Kuhi-lal rocks may have been substantially less.
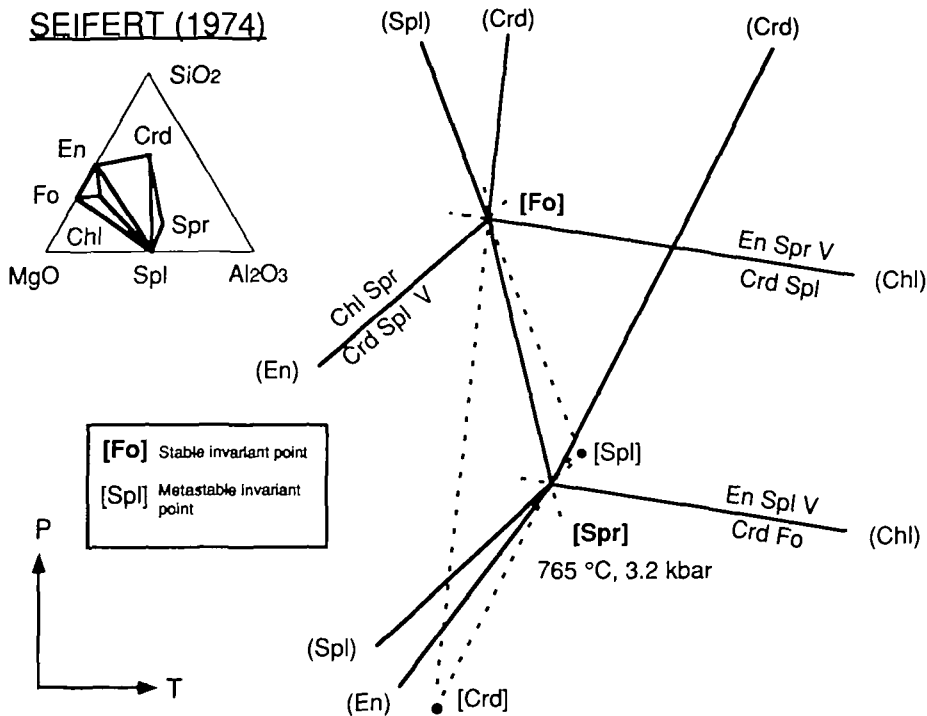
FIG. 8. Diagram simplified from a portion of Seifert's (1974, fig. 11) grid for the aluminous part of the system MgO–Al$_2$O$_3$–SiO$_2$–H$_2$O, in which Seifert's invariant points I_{18} and I_{16} correspond to [Fo] and [Spr], respectively. Slope of the reaction joining [Fo] and [Spr] is shown as negative for convenience of illustration; Seifert (1974) reported it to be near-vertical. Univariant equilibria are identified by the absent phase in parentheses; invariant points, by the absent phase in square brackets. Abbreviations as in Table 1, and V—vapor.

The six possible invariant points in the grid at $a_{H_2O} = 1$ are the intersections of six univariant lines in P–T–a_{H_2O} space with the plane corresponding to $a_{H_2O} = 1$. The six univariant lines meet at an invariant point involving all six phases at some a_{H_2O} less than unity (a_i, Fig. 9). Intersection of the univariant lines with a plane corresponding to an $a_{H_2O} < a_i$ will result in a P–T grid (six-phase multisystem), which Korzhinskii (1957, figs. 81 and 85) referred to as the 'second variant' and Zen (1966) as the 'residual system' for the grid at $a_{H_2O} = 1$. One variant is obtained from the other by rotating the array of univariant curves 180° and making the stable invariant points metastable and vica versa. Hensen's (1986, fig. 2) construction implies that either variant could be applicable to a given natural system, one at low activities of a mobile component, the other at high activities of this component.

P–T–a_{H_2O} conditions for Spr + Fo stability

The grid at $a_{H_2O} < 1$ has a stability field for Spr + Fo (Fig. 10). The maximum pressures for Spr + Fo are constrained by the reaction En + Spl = Fo + Spr, whose position in P–T space is independent of a_{H_2O}. Its slope is calculated to be very gently positive (Table 6), and the ΔV at 298·15 K changes little with increasing Al$_2$O$_3$ content of enstatite [using molar volumes of aluminous enstatite from Danckwerth & Newton (1978)]. Extrapolations of Seifert's (1974) reactions suggest that En + Spl = Fo + Spr could lie at 3–4 kbar for T near 700 °C. Using GE$\emptyset$-CALC (Berman et al., 1987) for the reaction (Spr, Crd) assuming an enstatite variable
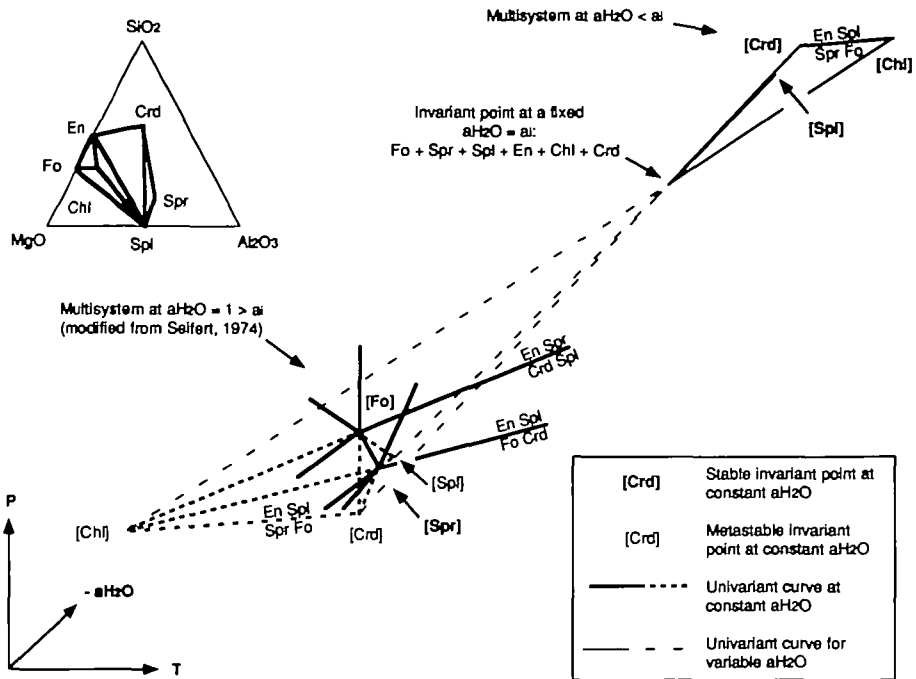
FIG. 9. Schematic diagram for the system $MgO-Al_2O_3-SiO_2-H_2O$ illustrating the relationship between Seifert's (1974) multisystem based on experiments at $a_{H_2O}=1$ and the multisystem at low a_{H_2O} using the construction suggested by Hensen (1986, fig. 2). We have illustrated only two or three of the five univariant equilibria around [Spl] and [Chl] and five of the six invariant points in the system at $a_{H_2O}=1$, three of the six univariant curves for variable a_{H_2O}, and a small portion of the system at low a_{H_2O}. For simplicity, we have shown the equilibria involving enstatite as straight lines with positive slopes; this should be valid for $T \leqslant 750\,°C$. Invariant points are identified by the absent phase in square brackets. Abbreviations as in Table 1, and Crd—cordierite.

in Al and hydrous cordierite, the [Crd] invariant point in Fig. 10 is calculated to be at 710 °C and $P \approx 4·0$ kbar for $a_{H_2O}=0·8$, and at 630 °C and $P \approx 3·7$ kbar for $a_{H_2O}=0·4$.

Harley & Hensen's (1990) estimate of 850 °C, 5 kbar for the Napier Mountains, Antarctica (Table 1), is not inconsistent with our estimated maximum of 4 kbar for Spr + Fo. Enstatite is absent from the sapphirine + forsterite assemblage in the marble from the Mojave Desert, California (Henry & Dokka, 1992), and thus the 4-kbar upper limit imposed by the reaction En + Spl = Spr + Fo (Fig. 10) does not apply. Consequently, Henry & Dokka's (1992) pressure estimate of 7·5–9 kbar for sapphirine + forsterite does not contradict the conclusions presented here.

The cordierite-free assemblage in sample KL920A suggests that the *P–T* path for Kuhi-lal passed close to [Crd], that is, neat $T \approx 650\,°C$ and $P \approx 4$ kbar for $a_{H_2O} \approx 0·5$. At this low a_{H_2O}, the En + Spl assemblage was succeeded during decompression by the Spr + Fo assemblage instead of the Crd + Fo assemblage predicted by Seifert's (1974) experiments at $a_{H_2O}=1$. However, the 4-kbar estimate is less than the 6·2–6·5 kbar pressures which Grew *et al.* (1988) inferred for the decompression event at Kuhi-lal. The 6·2–6·5-kbar estimate was based on data reported in the literature for other localities in the southwestern Pamirs, and Grew *et al*'s (1988) assumption that it applied to the decompression event could be in error. Chinner & Schairer's (1962) and Seifert's (1974) experimental results imply that the cordierite + anorthite + corundum ± sapphirine coronas in the whiteschists could have been stable at the 4-kbar maximum pressure inferred here for sapphirine + forsterite.
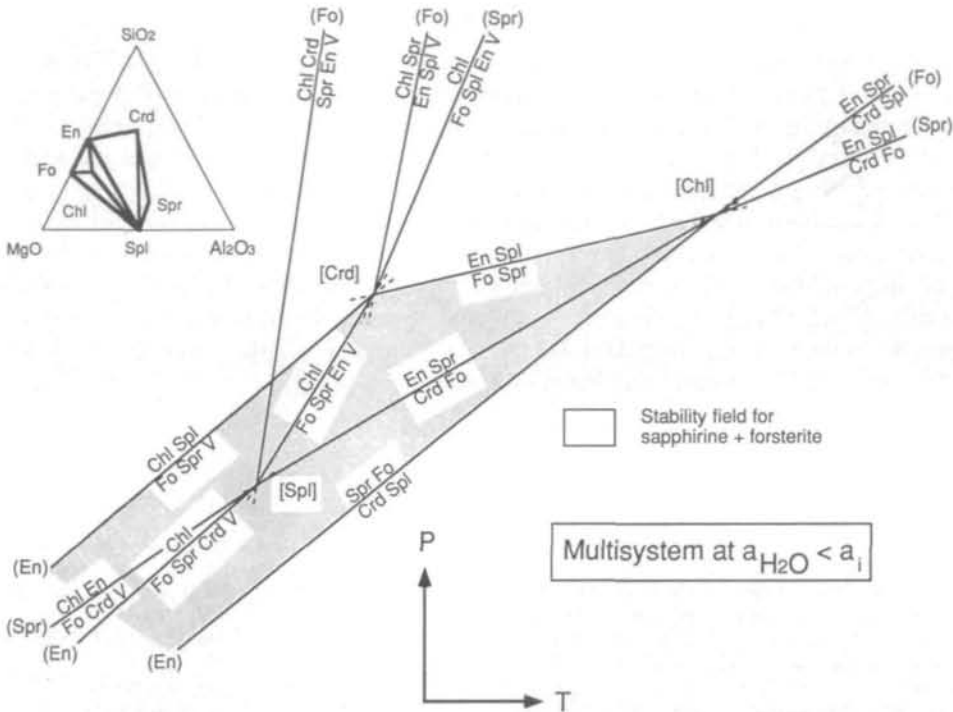
FIG. 10. Multisystem for an a_{H_2O} less than the a_i shown in Fig. 9 illustrating a stability field for sapphirine + forsterite in the system $MgO-Al_2O_3-SiO_2-H_2O$. For simplicity, we have shown the equilibria involving enstatite as straight lines with positive slopes; this should be valid for $T \leqslant 750\,°C$. Invariant points are identified by the absent phase in square brackets. Abbreviations as in Table 1, and Crd—cordierite, V—vapor.

TABLE 6

Molar entropies and volumes used in calculations of the reaction $9\,Spinel +$ $8\,Enstatite \rightarrow 5\,Forsterite + Sapphirine$ (at P = 1 bar)

	S J/mol K 298·15 K	S J/mol K 1000 K	V J/bar 298·15 K	V J/bar 1000 K
Spinel*	84·535	268·852	3·977	4·047
Enstatite*	66·170	196·410	3·133	3·199
Forsterite*	94·010	276·146	4·366	4·475
Sapphirine†	—	2611·8	39·589	40·290
Δ	—	+1·58	+0·56	+0·65

* The 298·15 K values were taken from Berman (1988); 1000 K values were calculated using the coefficients and equations (3)–(5) of Berman (1988) and assuming En = MgSiO₃.

† Volume for composition $Mg_7Al_{18}Si_3O_{40}$ at 298·15 K was taken from Newton *et al.* (1974). Volume at 1000 K was calculated using the same coefficients as for spinel. The molar entropy was taken from Waters (1986), who calculated this value from Seifert's (1974) data.

ACKNOWLEDGEMENTS

REFERENCES

Bence, A. E., & Albee, A. L., 1968. Empirical correction factors for the electron microanalysis of silicates and oxides. *J. Geol.* **76,** 382–403.

Berman, R. G., 1988. Internally-consistent thermodynamic data for minerals in the system $Na_2O-K_2O-CaO-MgO-FeO-Fe_2O_3-Al_2O_3-SiO_2-TiO_2-H_2O-CO_2$. *J. Petrology* **29,** 445–522.

—— Brown, T. H., & Perkins, E. H., 1987. GEØ-CALC: Software for calculation and display of *P-T-X* phase diagrams. *Am. Miner.* **72,** 861–2.

Budanova, K. T., 1987. Whiteschists and their connection with Precambrian evaporitic metasediments (for example, the southern Pamirs). *Dokl. Akad. Nauk Tadzhik. SSR* **30**(8), 515–20 (in Russian).

Chinner, G., & Schairer, J. F., 1966. The join $Ca_3Al_2Si_3O_{12}-Mg_3Al_2Si_3O_{12}$ and its bearing on the system $CaO-MgO-Al_2O_3-SiO_2$ at atmospheric pressure. *Am. J. Sci.* **260,** 611–34.

Christy, A. G., Phillips, B. L., Güttler, B. K., & Kirkpatrick, R. J., 1992. A ^{27}Al and ^{29}Si MAS NMR and infrared spectroscopic study of Al–Si ordering in natural and synthetic sapphirine. *Am. Miner.* **77,** 8–18.

Danckwerth, P. A., & Newton, R. C., 1978. Experimental determination of the spinel peridotite to garnet peridotite reaction in the system $MgO-Al_2O_3-SiO_2$ in the range 900°–1100°C and Al_2O_3 isopleths of enstatite in the spinel field. *Contr. Miner. Petrol.* **66,** 189–201.

Deer, W. A., Howie, R. A., & Zussman, J., 1978. *Rock-forming Minerals*, Vol. 2A, *Single-Chain Silicates*, 2nd ed. New York: John Wiley, 668 pp.

—— —— —— 1982. *Rock-forming Minerals*, Vol. 1A, *Orthosilicates*, 2nd ed. Harlow, Essex: Longman, 919 pp.

Desio, A., 1975. Geology of central Badakhshan (North-east Afghanistan) and surrounding countries. *Italian Expeditions to the Karakorum (K^2) and Hindu Kush, Sci. Rep., Part III, Vol. 3, Geology–Petrology.* Leiden: E. J. Brill, 628 pp.

—— Martina, E., & Pasquarè, G., 1964. On the geology of central Badakhshan (north-east Afghanistan). *Q. J. Geol. Soc. Lond.* **120,** 127–51.

Drugova, G. M., Moskovchenko, N. I., Sedova, I. S., & Miller, Yu. V., 1976. Metamorphic evolution in the basement of Phanerozoic fold zones (for example, the southwestern Pamirs). In: *The Thermodynamic Regime of Metamorphism.* Leningrad: Nauka, pp. 240–51 (in Russian).

Foster, W. R., 1950. Synthetic sapphirine and its stability relations in the system $MgO-Al_2O_3-SiO_2$. *J. Geol.* **58,** 135–51.

Grew, E. S., 1981. Surinamite, taaffeite, and beryllian sapphirine from pegmatites in granulite-facies rocks in Casey Bay, Enderby Land, Antarctica. *Am. Miner.* **66,** 1022–33.

—— 1988. Kornerupine at the Sar-e-Sang, Afghanistan, whiteschist locality: implications for tourmaline-kornerupine distribution in metamorphic rocks. *Ibid.* **73,** 345–57.

—— Belakovskiy, D. I., & Leskova, N. V., 1988. Phase equilibria in talc–kyanite–hornblende rocks (with andalusite and sillimanite) from Kuhi-lal, southwestern Pamirs. *Dokl. Akad. Nauk SSSR* **299,** 1222–6 (in Russian).

—— Chernosky, J. V., Werding, G., Abraham, K., Marquez, N., & Hinthorne, J. R., 1990*a*. Chemistry of kornerupine and associated minerals, a wet chemical, ion microprobe, and X-ray study emphasizing Li, Be, B and F contents. *J. Petrology* **31,** 1025–70.

—— Litvinenko, A. K., & Pertsev, N. N., 1990*b*. In search of whiteschists and kornerupine in the southwestern Pamirs, USSR. *Episodes* **13,** 270–4.

—— Pertsev, N. N., Yates, M. G., & Marquez, N., 1991. Sapphirine + forsterite and sapphirine + humite group minerals in an ultramagnesian lens from Kuhi-lal, SW Pamirs, USSR: Are these assemblages forbidden? *Geol. Soc. Am. Abstr. Prog.* **23**(5), A444.

Harley, S. L., & Hensen, B. J., 1990. Archaean and Proterozoic high-grade terranes of East Antarctica (40–80°E): a case study of diversity in granulite facies metamorphism. In: Ashworth, J. R., & Brown, M. (eds.) *High-temperature Metamorphism and Crustal Anatexis. Mineralogical Society Series*, **2**. London: Unwin Hyman, 320–70.

Henry, D. J., & Dokka, R. K., 1992. Metamorphic evolution of exhumed middle to lower crustal rocks in the Mojave Extensional Belt, southern California, USA. *J. Metamorphic Geol.* **10**, 347–64.

Hensen, B. J., 1986. Theoretical phase relations involving cordierite and garnet revisited: the influence of oxygen fugacity on the stability of sapphirine and spinel in the system Mg–Fe–Al–Si–O. *Contr. Miner. Petrol.* **92**, 362–7.

—— Essene, E. J., 1971. Stability of pyrope–quartz in the system $MgO–Al_2O_3–SiO_2$. *Ibid.* **30**, 72–83.

Herzberg, C. T., 1983. The reaction forsterite + cordierite = aluminous orthopyroxene + spinel in the system $MgO–Al_2O_3–SiO_2$. *Ibid.* **84**, 84–90.

Keith, M. L., & Schairer, J. F., 1952. The stability field of sapphirine in the system $MgO–Al_2O_3–SiO_2$. *J. Geol.* **60**, 181–6.

Kiselyov, V. I., & Budanov, V. I., 1986. *Precambrian Magnesian Skarn Deposits of the Southwestern Pamirs*. Donish: Dushanbe, 224 pp. (in Russian).

Kiselyova, I. A., 1976. Thermodynamic parameters of natural ordered sapphirine and synthetic disordered specimens. *Geokhimiya* **1976**(2), 189–201. (English translation *Geochem. Int.* **13**(1), 113–22.)

Korzhinskii, D. S., 1957. *Physicochemical Basis of the Analysis of Parageneses of Minerals*. Nauka: Moscow, 182 pp. (in Russian). (English translation, 1959, New York: Consultants Bureau.)

Kulke, H., & Schreyer, W., 1973. Kyanite–talc schist from Sar e Sang, Afghanistan. *Earth Planet. Sci. Lett.* **18**, 324–8.

Lal, R. K., Ackermand, D., Seifert, F., & Haldar, S. K., 1978. Chemographic relationships in sapphirine-bearing rocks from Sonapahar, Assam, India. *Contr. Miner. Petrol.* **67**, 169–87.

Liu, T.-C., & Presnall, D. C., 1990. Liquidus phase relationships on the join anorthite–forsterite–quartz at 20 kbar with applications to basalt petrogenesis and igneous sapphirine. *Ibid.* **104**, 735–42.

Massonne, H.-J., 1989. The upper thermal stability of chlorite + quartz: an experimental study in the system $MgO–Al_2O_3–SiO_2–H_2O$. *J. Metamorphic Geol.* **7**, 567–81.

Newton, R. C., Charlu, T. V., & Kleppa, O. J., 1974. A calorimetric investigation of the stability of anhydrous magnesium cordierite with application to granulite facies metamorphism. *Contr. Miner. Petrol.* **44**, 295–311.

Ravich, M. G., & Kamenev, Ye. N., 1972. *Crystalline Basement of the Antarctic Platform*. Leningrad: Gidrometeoizdat, 658 pp. (in Russian). (English translation, 1975, New York: John Wiley, 582 pp.)

Sahama, T. G., Lehtinen, M., Rehtijärvi, P., & von Knorring, O., 1974. Properties of sapphirine. *Ann. Acad. Sci. Fenn., Series A, III* **114**, 1–24.

Schreyer, W., 1977. Whiteschists: their compositions and pressure–temperature regimes based on experimental, field, and petrographic evidence. *Tectonophysics* **43**, 127–44.

—— Abraham, K., 1976. Three-stage metamorphic history of a whiteschist from Sar e Sang, Afghanistan, as part of a former evaporite deposit. *Contr. Miner. Petrol.* **59**, 111–30.

—— Schairer, J. F., 1961. Compositions and structural states of anhydrous Mg-cordierites: a re-investigation of the central part of the system $MgO–Al_2O_3–SiO_2$. *J. Petrology* **2**, 324–406.

Seifert, F., 1974. Stability of sapphirine: a study of the aluminous part of the system $MgO–Al_2O_3–SiO_2–H_2O$. *J. Geol.* **82**, 173–204.

Shanin, L. L., Volkov, V. N., Litsarev, M. A., Arakelyants, M. M., Gol'tsman, Yu. V., Ivanenko, V. V., & Bairova, E. D., 1979. *Criteria for Reliability of Radiological Dating Methods*. Moscow: Nauka, 208 pp. (in Russian).

Smart, R. M., & Glasser, F. P., 1976. Phase relations of cordierite and sapphirine in the system $MgO–Al_2O_3–SiO_2$. *J. Mater. Sci.* **11**, 1459–64.

Taylor, H. C. J., 1973. Melting relations in the system $MgO–Al_2O_3–SiO_2$ at 15 kb. *Geol. Soc. Am. Bull.* **84**, 1335–48.

Vlasov, N. G., & D'yakov, Yu. A., 1989. Geological map of the Tajik SSR and contiguous territories. Leningrad: USSR Ministry of Geology, PO 'Tajikgeologiya', and All-Union Scientific Research Geological Institute (VSEGEI), scale 1:500 000 (in Russian).

Waters, D. J., 1986. Metamorphic history of sapphirine-bearing and related magnesian gneisses from Namaqualand, South Africa. *J. Petrology* **27**, 541–65.

Zen, E., 1966. Some topological relationships in multisystems of $n + 3$ phases I. General theory; unary and binary systems. *Am. J. Sci.* **264**, 401–27.

Zotov, I. A., 1966. A find of sapphirine in the magnesian skarns of the southwestern Pamirs. *Dokl. Akad. Nauk SSSR* **170**, 684–7 (in Russian). (English translation: *Dokl. Acad. Sci. USSR, Earth Sci. Sect.* **170**, 146–8.)

—— Sidorenko, G. A., 1968. Magnesian gedrite from the southwestern Pamirs. *Dokl. Akad. Nauk SSSR* **180**, 700–3 (in Russian). (English translation: *Dokl. Acad. Sci. USSR, Earth Sci. Sect.* **180**, 138–41.)